



# N,N-Dimethylformamide Delays LPS-Induced Preterm Birth in a Murine Model by Suppressing the Inflammatory Response

Zeng-Hui Wei<sup>1</sup> · Oluwabukola O. Salami<sup>1</sup> · Jagadish Koya<sup>1</sup> · Swapna Munnangi<sup>2</sup> · Ryan Pekson<sup>3</sup> · Charles R. Ashby Jr<sup>1</sup> · Sandra E. Reznik<sup>1,4</sup>

Received: 25 October 2021 / Accepted: 11 March 2022 / Published online: 29 March 2022  
© Society for Reproductive Investigation 2022

## Abstract

Preterm birth accounts for the majority of perinatal mortality worldwide, and there remains no FDA-approved drug to prevent it. Recently, we discovered that the common drug excipient, N,N-dimethylacetamide (DMA), delays inflammation-induced preterm birth in mice by inhibiting NF- $\kappa$ B. Since we reported this finding, it has come to light that a group of widely used, structurally related aprotic solvents, including DMA, N-methyl-2-pyrrolidone (NMP) and dimethylformamide (DMF), have anti-inflammatory efficacy. We show here that DMF suppresses LPS-induced TNF $\alpha$  secretion from RAW 264.7 cells and IL-6 and IL-8 secretion from HTR-8 cells at concentrations that do not significantly affect cell viability. Like DMA, DMF protects I $\kappa$ B $\alpha$  from degradation and prevents the p65 subunit of NF- $\kappa$ B from translocating to the nucleus. *In vivo*, DMF decreases LPS-induced inflammatory cell infiltration and expression of TNF $\alpha$  and IL-6 in the placental labyrinth, all to near baseline levels. Finally, DMF decreases the rate of preterm birth in LPS-induced pregnant mice ( $P < .0001$ ) and the rate at which pups are spontaneously aborted ( $P < .0001$ ). In summary, DMF, a widely used solvent structurally related to DMA and NMP, delays LPS-induced preterm birth in a murine model without overt toxic effects. Re-purposing the DMA/DMF/NMP family of small molecules as anti-inflammatory drugs is a promising new approach to delaying or reducing the incidence of inflammation-induced preterm birth and potentially attenuating other inflammatory disorders as well.

**Keywords** Preterm Birth · N,N-Dimethylformamide · N,N-Dimethylacetamide · Inflammation

## Introduction

Preterm birth (PTB) is the leading cause of neonatal morbidity and mortality worldwide [1, 2]. Fifteen million babies are born preterm each year, and among industrialized nations, the USA has the highest rate of PTB [2]. Children born prematurely have an increased risk of developing neurological, respiratory and metabolic abnormalities

[3], including metabolic syndrome [4, 5]. Although spontaneous PTB results from multiple causes, including oxidative stress, dysbiosis [6, 7] and secretion of exosomes [8, 9], inflammation, whether in the absence or presence of infection, accounts for most cases of spontaneous PTB [10]. The one drug that was conditionally approved by the United States Food and Drug Administration (FDA) to prevent PTB, 17-hydroxyprogesterone caproate [11, 12], produced variable results and was intended only as a prophylactic agent, not for women in active labor [13]. Furthermore, this drug is ineffective in the following types of patients: 1) women with multiple gestation pregnancies [13], 2) obese women [14, 15] and 3) African-American women [16, 17]. Groups 2 and 3 are particularly concerning, because one in five pregnant women will be overweight by 2025 [18] and African-Americans have the highest rate of PTB [19]. Finally, based on the results of the follow-up double-blind randomized (PROLONG) clinical trial, showing that 17-hydroxyprogesterone caproate has no significant efficacy

✉ Sandra E. Reznik  
rezniks@stjohns.edu

<sup>1</sup> Department of Pharmaceutical Sciences, St. John's University, Queens, NY, USA

<sup>2</sup> Department of Surgery, Nassau University Medical Center, Nassau, NY, USA

<sup>3</sup> Departments of Cell Biology and Medicine, Albert Einstein College of Medicine, Bronx, NY, USA

<sup>4</sup> Departments of Pathology and Obstetrics & Gynecology and Women's Health, Albert Einstein College of Medicine, Bronx, NY, USA

in preventing PTB when compared to a placebo [20], the FDA has withdrawn approval of this agent to prevent PTB.

We and others have recently discovered that the common drug excipient, N,N-dimethylacetamide (DMA), and related compounds have anti-inflammatory efficacy [21–24]. We were the first to report that DMA inhibits nuclear factor kappa light-chain enhancer of activated B cells (NF- $\kappa$ B) nuclear translocation and protects nuclear factor of kappa light polypeptide gene enhancer in B-cells inhibitor, alpha (I $\kappa$ B $\alpha$ ) from degradation [21]. Although it has been reported that DMA attenuates osteoporosis [23] and enhances bone healing impeded by inflammation [24] in *in vivo* models, we were the first to demonstrate that DMA has tocolytic activity. Interestingly, while our previous results indicated that monomethylacetamide (the primary metabolite of DMA) has no anti-inflammatory efficacy [22], N,N-dimethylformamide (DMF), which substitutes a hydrogen atom at the C-methyl location, is a novel cytokine suppressive anti-inflammatory compound, similar to DMA. In this work, we conducted experiments to determine whether DMF has tocolytic as well as anti-inflammatory efficacy and whether it acts via the same mechanism as DMA.

## Methods

### Cell Viability Assays

RAW 264.7 cells were obtained from the American Type Culture Collection (Manassas, VA) and maintained in Dulbecco's modified Eagle medium supplemented with 10% FBS and 1% penicillin–streptomycin as described [22]. HTR-8/SVneo cells (HTR-8 cells) were kindly donated by Dr. Charles Graham (Queens's University, Ontario, Canada) and grown in Roswell Park Memorial Institute (RPMI) medium (Cellgro, Corning, NY) supplemented with 10% FBS and 1% penicillin–streptomycin. All cells were maintained at 37°C and 5% CO<sub>2</sub> and allowed to grow to 80–90% confluency before being sub-cultured or used in experiments. Cells were seeded at 20,000 cells per well in 96-well plates and pre-incubated with N,N-dimethylformamide (DMF, Sigma–Aldrich, St. Louis, MO) (0.1 to 40 mM) for 2 h and then incubated with 1  $\mu$ g/ml of LPS (*Escherichia coli* 026:B6, Sigma, St. Louis, MO) for 24 h. Negative controls with no DMF and negative controls with no LPS were also included. At the end of the 24-h incubation, 3-(4,5-dimethyl thiazolyl-2)-2,5-diphenyl tetrazolium bromide (MTT, Alfa Aesar, Ward Hill, MA) was added to each well at a final concentration of 5.0 mg/ml. After incubation for 2 h at 37°C and 5% CO<sub>2</sub>, the media were aspirated and dimethyl sulfoxide (DMSO) (100  $\mu$ l/well) (BDH, Radnor, PA) was added to dissolve formed purple formazan crystals. The plates were shaken on an orbital microplate shaker for 10 min to ensure

complete solubilization of the crystals, and the absorbance of the resulting purple solution was measured at 570 nm using an Opsys MR microplate reader (Dynex Technologies, Chantilly, VA). Three independent experiments were performed in duplicate for each cell line.

### Enzyme-Linked Immunosorbent Assay

RAW 264.7 and HTR-8 cells were grown in the presence of DMF (0.1 to 30 mM) for 2 h and then incubated with LPS (1  $\mu$ g/ml) for another 24 h. Negative controls with no DMF and negative controls with no LPS were also included. BAY 11-7082 (5  $\mu$ M) was included as a positive control. The levels of tumor necrosis alpha (TNF $\alpha$ ), interleukin (IL)-6, IL-8 and monocyte chemoattractant protein (MCP)-1 in the supernatants were determined using Ready-SET-Go! sandwich ELISA kits (eBioscience, San Diego, CA) as per the manufacturer's protocol. The ELISA for each experimental sample was performed in duplicate. Three independent experiments were performed in duplicate for each cytokine.

### Western Blotting

To determine the effect of DMF on various proteins such as I $\kappa$ B $\alpha$  and native and phosphorylated forms of p38 mitogen-activated protein (MAP) kinase, extracellular signal-regulated kinase (ERK) and c-jun N-terminal kinase (JNK), RAW 264.7 cells were seeded at  $1.5 \times 10^6$  cells per 25-cm<sup>2</sup> flasks and allowed to grow for 48 h at 37°C and 5% CO<sub>2</sub>. The cells were incubated for 2 h in the absence or presence of DMF (10, 20 and 30 mM). For the determination of I $\kappa$ B $\alpha$  and the native and phosphorylated forms of p38, ERK and JNK, cells were stimulated with LPS (1  $\mu$ g mL<sup>-1</sup>) for 15 min. Whole cell lysates were prepared using a modified protocol as described by Abcam. Briefly, cells were lysed in radio immunoprecipitation assay (RIPA) lysis buffer (G Biosciences, St. Louis, MO) freshly supplemented before use with 1 mM of phenylmethylsulfonyl fluoride and ethylenediaminetetraacetic acid-free protease inhibitor cocktail set III (Calbiochem, San Diego, CA) by repeated vortexing on ice for 30 min. Samples were then centrifuged at 14,000  $\times$  g for 20 min at 4°C, and supernatants were collected as whole cell lysates. Protein concentrations of the samples were determined using bicinchoninic acid (BCA) protein assay (Thermo Fisher, Waltham, MA). Equal amounts of total protein were resolved in 10% SDS–PAGE and transferred onto PVDF membranes (Bio-Rad, Hercules, CA). The membranes were blocked for 2 h at room temperature using 5% skimmed milk in TBST [20 mM Tris (pH 7.6), 150 mM NaCl, 0.1% Tween 20] and incubated at 4°C overnight with a 1:1,000 dilution of primary antibody for glyceraldehyde-3-phosphate dehydrogenase (GAPDH, gel loading control), p38, p-p38, ERK 1/2, p-ERK1/2, JNK, p-JNK

(Cell Signaling Technologies, Danvers, MA) or  $\text{I}\kappa\text{B}\alpha$  (Santa Cruz, Dallas, TX). The membranes were washed with TBST and then incubated at room temperature for one h with a 1:1,000 dilution of horseradish peroxidase-linked secondary antibody (GE Healthcare, Pittsburgh, PA) in 5% skimmed milk. Protein expression was detected using Pierce enhanced chemiluminescence (Thermo Fisher, Waltham, MA), developed with clear blue X-ray films (Thermo Fisher, Waltham, MA) and analyzed using ImageJ software (NIH, Bethesda, MD). Three independent experiments were performed in duplicate.

## Immunofluorescence

To determine the effect of DMF on LPS-induced NF- $\kappa$ B nuclear translocation, RAW 264.7 cells were seeded and grown as above and incubated for two h in the absence or presence of 30 mM DMF and then for another 15 min in the absence or presence of 1  $\mu\text{g}/\text{ml}$  LPS. The cells were fixed with 4% paraformaldehyde for 15 min at room temperature after washing with ice-cold PBS. Cells were then permeabilized with 0.25% Triton X-100 for 15 min and blocked with 6% bovine serum albumin (BSA) in PBS for 1 hour at 37 °C. Fixed cells were incubated with monoclonal antibody against the NF- $\kappa$ B p65 protein (1:200) (Cell Signaling Technologies) overnight at 4 °C. Thereafter, the cells were further incubated with Alexa flour 488 donkey anti-rabbit IgG (1:400) (Invitrogen, Waltham, MA) for 2 h at 37 °C. To visualize the nuclei, cells were counterstained with 4',6-diamidino-2-phenylindole (DAPI) after rinsing with PBS. The immunofluorescence images were generated using a Nikon TE-2000S fluorescence microscope (Nikon Instruments Inc.).

## In Vivo Model

Eight-week-old C57Bl/6 mice were purchased from Taconic Biosciences (Rensselaer, NY) and housed at  $23 \pm 1^\circ\text{C}$  and humidity of  $50 \pm 10\%$  in the vivarium on a 12:12-h light/dark cycle. All experimental protocols were approved by the St. John's University Institutional Animal Care and Use Committee (IACUC) and are reported in accordance with ARRIVE guidelines (<https://arriveguidelines.org>).

A total of 21 timed pregnant dams at E15.5 were randomly divided into four groups: 1) the LPS group ( $n=8$ ), which were injected intraperitoneally (i.p.) with 100  $\mu\text{L}$  of phosphate buffered saline (PBS) at  $t = -15$  min and 10 h and with 50 mg/kg LPS (serotype 026:B6) at  $t = 0$ ; 2) the DMF rescued group ( $n = 7$ ), which were injected i.p. with 2.6 g/kg DMF at  $t = -15$  min and 10 h and with 50 mg/kg LPS at  $t = 0$ ; 3) the sham group ( $n = 4$ ), which were injected i.p. with 100  $\mu\text{L}$  of PBS at  $t = -15$  min and 10 h and with 500  $\mu\text{L}$  of PBS at  $t = 0$ ; and 4) the DMF control group ( $n = 2$ ),

which were injected with 2.6 g/kg DMF at  $t = -15$  min and 10 h and with 500  $\mu\text{L}$  of PBS at  $t = 0$  (see Supplementary Table 1 for a summary of the mouse groups). In accordance with our IACUC's regulations, the mice were killed within 2 h of delivery, defined as the delivery of one pup, and the mice that had not gone into labor were euthanized at  $t = 24$  h. All mice were necropsied to confirm pregnancy, and the retained pups were counted and examined. Mice challenged with LPS and treated with DMA that did not deliver within 24 h were considered "rescued." Similarly, pups in litters from dams exposed to LPS and treated with DMA that were not delivered within 24 h were considered "rescued."

## Histological Analysis

One placenta was randomly selected from each dam, fixed in formalin, embedded in paraffin, sectioned at 4  $\mu\text{m}$  and stained with hematoxylin and eosin (H&E) as previously described [21, 25, 26]. Sections were examined under a Nikon Eclipse 80i light microscope (Nikon Inc., Melville, NY) by three blinded observers (OOS, SM and SER), one of whom is a practicing placental pathologist (SER). Sections were graded for degree of inflammatory cell infiltration on a four-point scale (Grades 0-3). Sections were initially scanned at a magnification of 100x to identify the three most active areas of inflammation. Each of those areas was then observed at 400x and graded based on the number of inflammatory cells per field as follows: Grade 0 = 0-5 cells, Grade 1 = 6-50 cells, Grade 2 = 51-100 cells and Grade 3 = more than 100 cells.

## Immunohistochemistry

The semiquantitative analysis and immunolocalization of TNF $\alpha$  and IL-6 in formalin-fixed paraffin-embedded mouse placental tissue sections were carried out using DAKO-Labeled Streptavidin-Biotin 2 System and horseradish peroxidase (LSAB2-system HRP, Dako, Carpinteria, CA), as previously described [25, 27]. Tissues were rehydrated and were immersed in citrate buffer (8.2 mmol/L sodium citrate and 1.8 mmol/L citric acid, pH 6.0, containing 0.01% Triton X-100), heated to 95°C - 98°C for 10 min and then cooled to room temperature to achieve antigen retrieval. Tissues were incubated in 3% hydrogen peroxide for 10 min to saturate native peroxidases and washed in PBS (Sigma-Aldrich) for 3 min. The sections were incubated in 1% bovine serum albumin in a humidified chamber for 90 min to reduce non-specific binding and then incubated overnight at 4°C with antibodies directed against TNF $\alpha$  or IL-6 (Sigma-Aldrich) diluted 1:100 in 1% BSA. The tissue sections were then washed in PBS for 10 min and incubated with secondary antibody biotinylated link for 1 h at room temperature in the humidified chamber, washed in Tris-buffered saline-Tween

and incubated with streptavidin–horseradish peroxidase for 10 min with subsequent washing in PBS for 3 min. The slides were developed using 3,3'-diaminobenzidine. The sections were observed under a Nikon Eclipse 80i light microscope at 400X magnification, and images were captured with SPOT Advanced Software and analyzed with Image-Pro Premier software (Media Cybernetics, Rockville, MD).

## Statistical Analysis

The MTT assay and ELISA data were analyzed with one-way analysis of variance (ANOVA) and Dunnett's test for post hoc analysis. The significance of the effect of DMF on the number of dams delivering prematurely and on the number of pups being prematurely delivered was determined using the Chi-square test and Fisher's exact test, respectively. The effect of DMF on dams delivering preterm, pups being delivered preterm and pup survival over the 24-h experimental period was analyzed using log-rank test (Mantel Cox). Differences in inflammatory cell infiltration in placentas harvested from the different mouse groups were analyzed using the Mann–Whitney U test, along with Tukey's multiple comparison *post hoc* analysis, using GraphPad Prism. The optical density of the immunohistochemical staining was determined by DAB analysis Image-Pro Premier software, and these data were exported to GraphPad Prism for statistical analysis using ANOVA and Tukey's post hoc test.

## Results

### DMF Inhibits Cytokine Secretion from RAW 264.7 and HTR-8 Cells

We first determined whether DMF inhibited the secretion of an acute-phase inflammatory cytokine in LPS-stimulated RAW 264.7 cells. No loss of cell viability was detected in RAW 264.7 cells incubated with concentrations of DMF from 0.1 to 30 mM (Supplementary Figure 1, A); therefore, concentrations of DMF up to 30 mM were used in this assay. As previously reported, LPS (1  $\mu\text{g/ml}$ ) increased the production of TNF $\alpha$  in RAW 264.7 cells approximately 18-fold ( $P < .0001$ , Figure 1, A). This effect was partially prevented by DMF in a concentration-dependent manner, with decreases in TNF $\alpha$  secretion of 19% ( $P < .01$ ) and 30% ( $P < .001$ ) in cells incubated with 20 and 30 mM DMF, respectively (Figure 1, A). Interestingly, DMF was at least as effective in reducing TNF $\alpha$  secretion as the NF- $\kappa$ B inhibitor BAY 11-7082, which was used as a positive control.

As placental trophoblast cells play an important role in inflammatory signaling at the maternal fetal interface [28], we next assessed DMF's effect on cytokine secretion in LPS-stimulated placental trophoblast HTR-8 cells. No loss

of cell viability was detected in HTR-8 cells incubated with concentrations of DMF from 0.1 to 10 mM (Supplementary Figure 1, B); therefore, concentrations of DMF up to 10 mM were used in this assay. LPS, at 1  $\mu\text{g/ml}$ , increased IL-6 secretion in HTR-8 cells more than fourfold ( $P < .001$ , Figure 1, B). DMF (0.1 to 10 mM) attenuated the LPS-induced increase in IL-6 in a concentration-dependent manner, with 10 mM DMF reducing IL-6 secretion by more than 40% ( $P < .05$ , Figure 1, B). The same concentration of LPS increased IL-8 secretion more than eightfold in HTR-8 cells (Figure 1, C). DMF attenuated this LPS-induced increase in IL-8 in a concentration-dependent manner as well, with 10 mM DMF reducing IL-8 secretion by 30% ( $P < .01$ , Figure 1, C). While LPS increased MCP-1 secretion in HTR-8 cells approximately fivefold, DMF had no statistically significant effect on MCP-1 (Figure 1, D). NF- $\kappa$ B inhibitor BAY 11-7082 was used as a positive control in all experiments (Figure 1, A–D).

### DMF Attenuates LPS-Induced Inflammatory Cell Infiltration of the Placental Labyrinth

Given DMF's effect on LPS-induced cytokine secretion *in vitro*, we hypothesized that it would decrease LPS-driven inflammatory cell infiltration *in vivo* in mouse placenta. Microscopic examination indicated a marked inflammatory cell infiltrate in the placental labyrinth in the LPS group compared to the sham group ( $P < .0001$ , Figure 2, B–D). This response, however, was significantly attenuated in placentas from the DMF rescued group ( $P < .0001$ , Figure 2, A, B and Figure D).

### DMF Attenuates LPS-Induced Increases in TNF $\alpha$ and IL-6 in the Placental Labyrinth

Immunohistochemical staining for TNF $\alpha$  in the placental labyrinth was increased almost fourfold in the LPS group as compared to the sham group ( $P < .0001$ , Figure 3, B–D). In contrast, immunohistochemical staining for TNF $\alpha$  was significantly reduced in the DMF rescued group compared to the LPS group ( $P < .0001$ , Figure 3, A, B and D) and, in fact, was similar to basal levels seen in the sham group (Figure 3, A, C and D). Similarly, immunohistochemical staining for IL-6 was increased approximately 20-fold in the LPS group compared to the sham group ( $P < .0001$ , Figure 4, B–D), whereas IL-6 was reduced by approximately 15-fold in the DMF rescued group compared to the LPS group ( $P < .0001$ , Figure 4, A, B and D).

### DMF Specifically Inhibits the NF- $\kappa$ B Pathway

To confirm that DMF acts on the NF- $\kappa$ B pathway in a similar manner as DMA, we tested DMF's effect on I $\kappa$ B $\alpha$

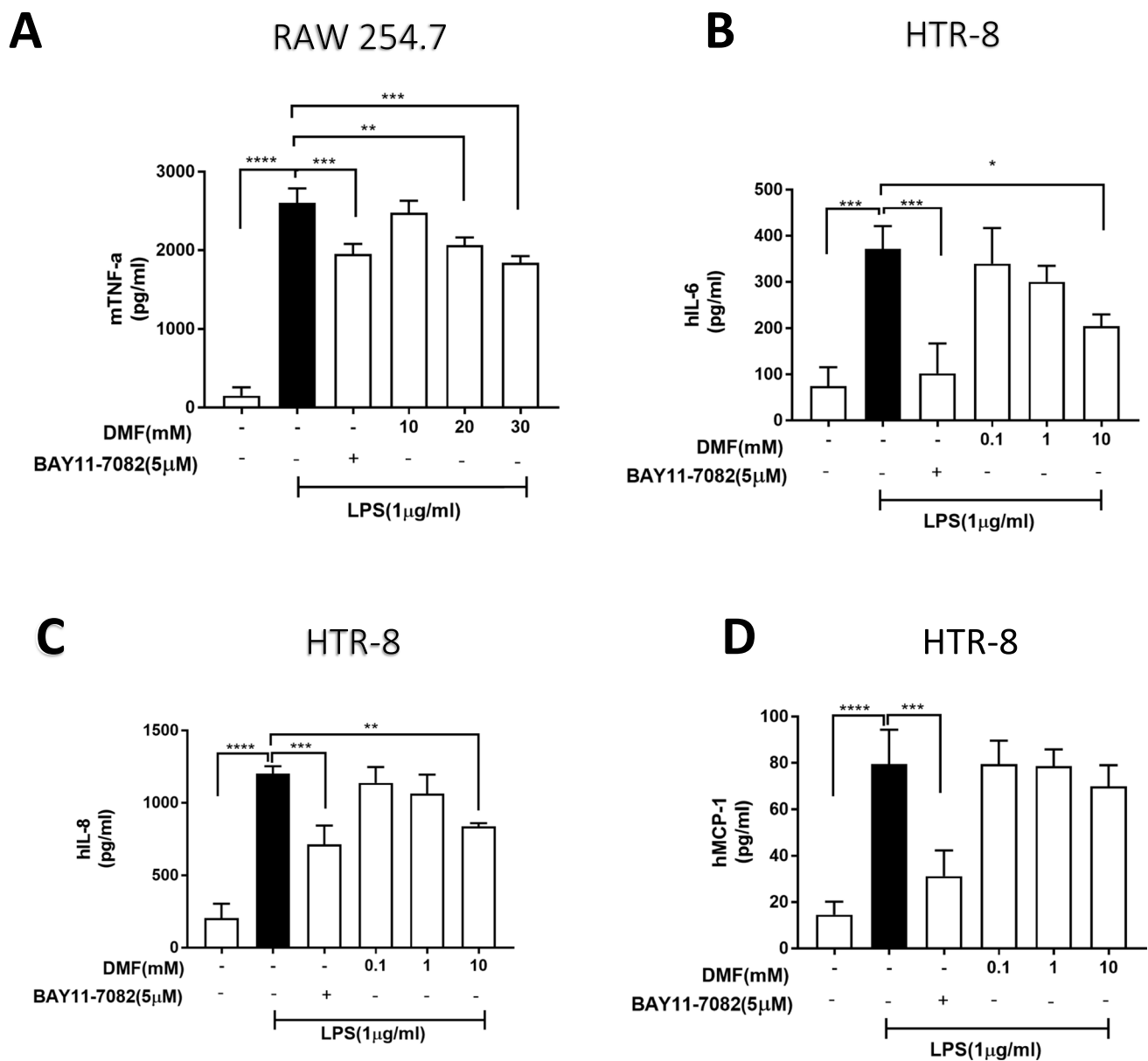


**Fig. 1** DMF suppresses cytokine secretion *in vitro*. **A**, RAW 264.7 cells or **B–D**, HTR-8 cells were stimulated with 1 μg/mL of LPS for 24 h in the absence or presence of various concentrations of DMF, which was added to the media 2 h before the LPS. Concentrations of **A**, TNFα, **B**, IL-6, **C**, IL-8 and **D**, MCP-1 in the media were determined by ELISA. BAY 11-7082 (5 μM) was included as a positive

control. The asterisk indicates  $P < .05$ ; the double asterisks indicate  $P < .01$ ; the triple asterisks indicate  $P < .001$ ; the quadruple asterisks indicate  $P < .0001$ . DMF, N,N-dimethylformamide; HTR-8, HTR-8/SVNeo; LPS, lipopolysaccharide; TNFα, tumor necrosis factor alpha; IL-6, interleukin-6; IL-8, interleukin-8; MCP-1, monocyte chemoattractant protein-1; ELISA, enzyme-linked immunosorbent assay

degradation. We performed these experiments with RAW 264.7 cells as macrophages are major regulators of inflammation and putative targets cells for DMF effects. As expected, LPS induced significant degradation of IκBα during a 15-min exposure ( $P < .0001$ , Figure 5, A). However, IκBα degradation was prevented by DMF in a concentration-dependent manner (Figure 4A). Data were normalized using GAPDH, and statistical analysis of the relative densities of IκBα revealed that the highest concentration of DMF (30

mM) significantly ( $P < 0.001$ ) inhibited IκBα degradation relative to the LPS control (Figure 5, B).

The effect of DMF on the expression and phosphorylation of proteins in the MAPK signaling pathways was evaluated in LPS-induced RAW 264.7 cells by western blotting of the phosphorylated and native forms of JNK, ERK1/2 and p38 MAPK (Figure 5, C). Bands for phosphorylated JNK, ERK1/2 and p38 MAPK (p-JNK, p-ERK1/2 and p-p38 MAPK, respectively) were seen 15 min after exposure to

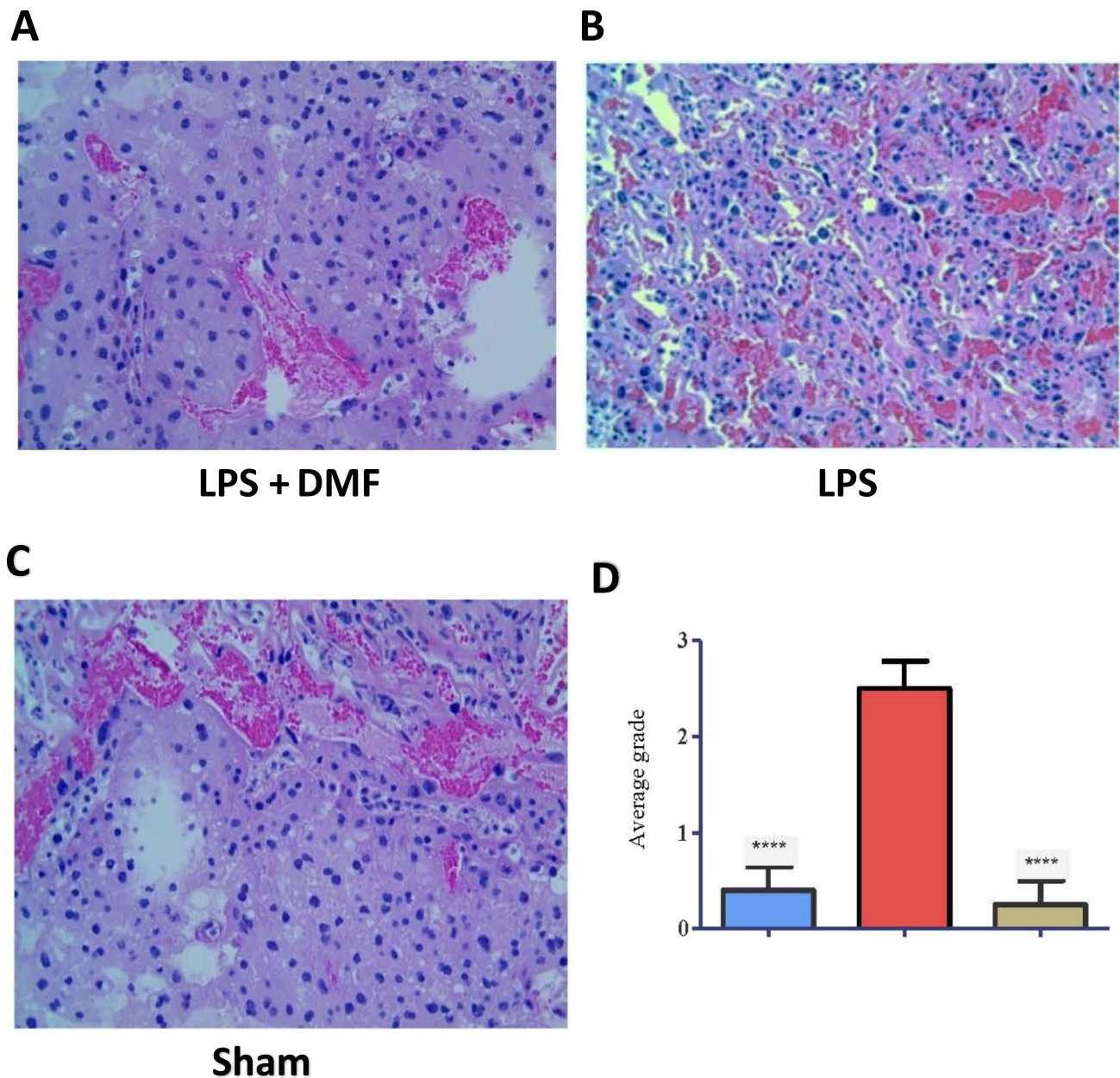


**Fig. 2** DMF suppresses inflammatory cell recruitment to the mouse placental labyrinth. One placenta per litter was randomly selected for histology from each of the **A**, DMA rescued (n=7); **B**, LPS (n=8); and **C**, sham (n=4) E16 dams. **A-C**, Representative H&E sections from each of the groups. **D**, Sections were graded for degree

of inflammatory cell infiltration on a four-point scale (Grades 0-3). Original magnification 400X. The *quadruple asterisks indicate*  $P < .0001$ , as compared to the LPS-challenged group. *DMF*, N,N-dimethylformamide; *LPS*, lipopolysaccharide

LPS (Figure 5, C, lane 2). In contrast, bands were barely detected or not detected in the untreated controls (Figure 5, C, lane 1). Incubating cells with increasing concentrations of DMF in the presence of LPS did not significantly change the expression of p-JNK, p-ERK1/2 or p-p38 MAPK (Figure 5, C, lanes 3-5) as compared to the controls. Similarly, the expression levels of the native forms of these proteins were not affected by DMF, as manifest by the uniform band densities across the treatment groups (Figure 5, C, lanes 3-5).

### DMF Inhibits Nuclear Translocation of NF- $\kappa$ B

As shown in the first row of Figure 6, immunoreactivity for the p65 subunit of NF- $\kappa$ B in unstimulated RAW 264.7 cells is primarily localized in the cytoplasm. Stimulation of the cells with 1  $\mu$ g/ml LPS for 15 minutes prompts translocation of the p65 subunit from the cytoplasm into the nucleus (Figure 6, second row). The presence of 30 mM DMF, however, causes some of the p65 to be retained in the cytoplasm,

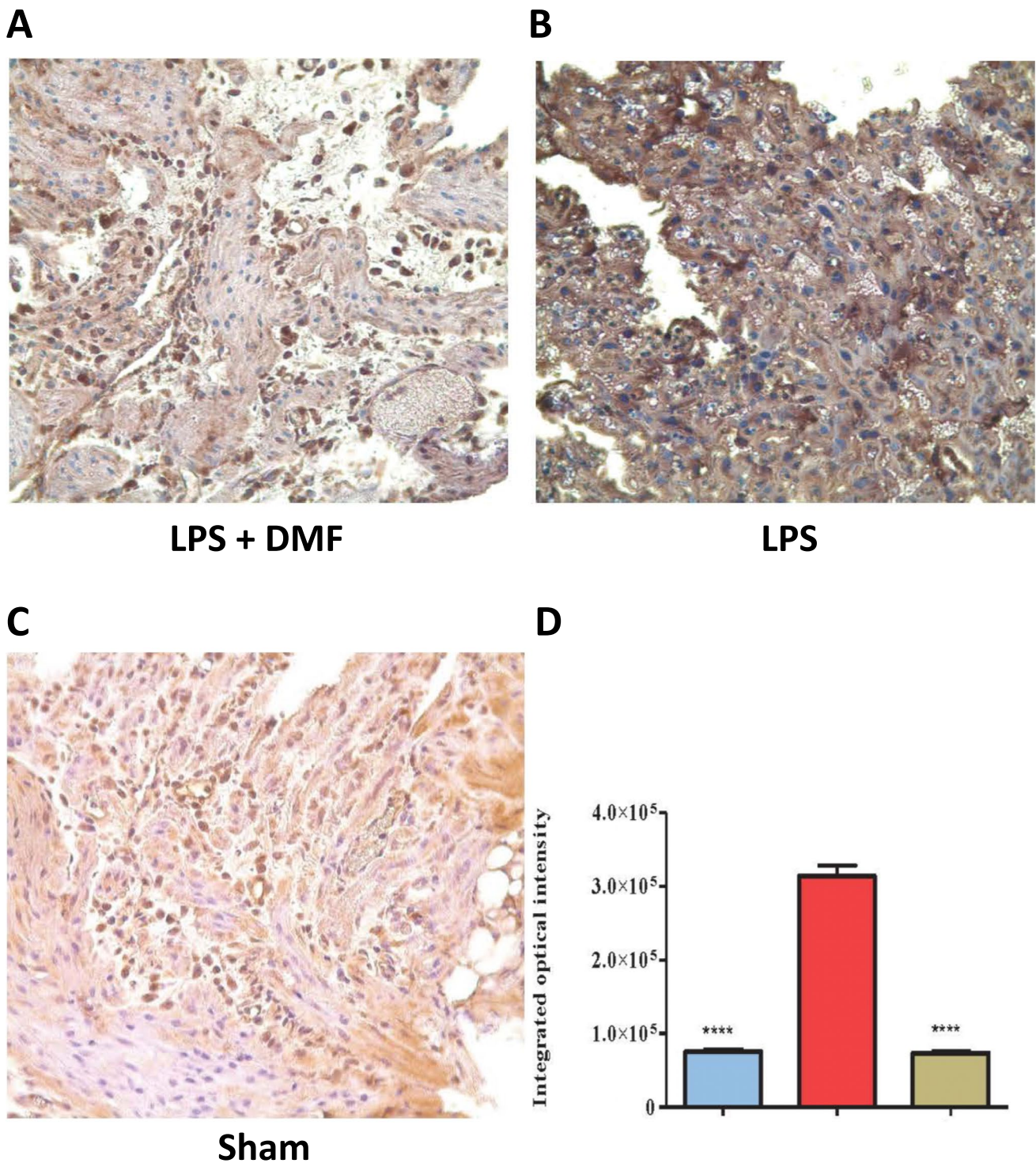


**Fig. 3** DMF attenuates TNF $\alpha$  expression in the mouse placental labyrinth. One placenta per litter was randomly selected for immunohistochemistry from each of the **A**, DMF rescued (n=7); **B**, LPS (n=8); and **C**, sham (n=4) E16 dams. **A-C**, Representative sections reacted with primary TNF $\alpha$  antibodies from each of the groups. **D**, Staining

intensity in the various groups, analyzed with Image-Pro Premier software. Original magnification 400X. The *quadruple asterisks* indicate  $P < .0001$ , as compared to the LPS group. *DMF*, N,N-dimethylformamide; *TNF $\alpha$* , tumor necrosis alpha; *LPS*, lipopolysaccharide

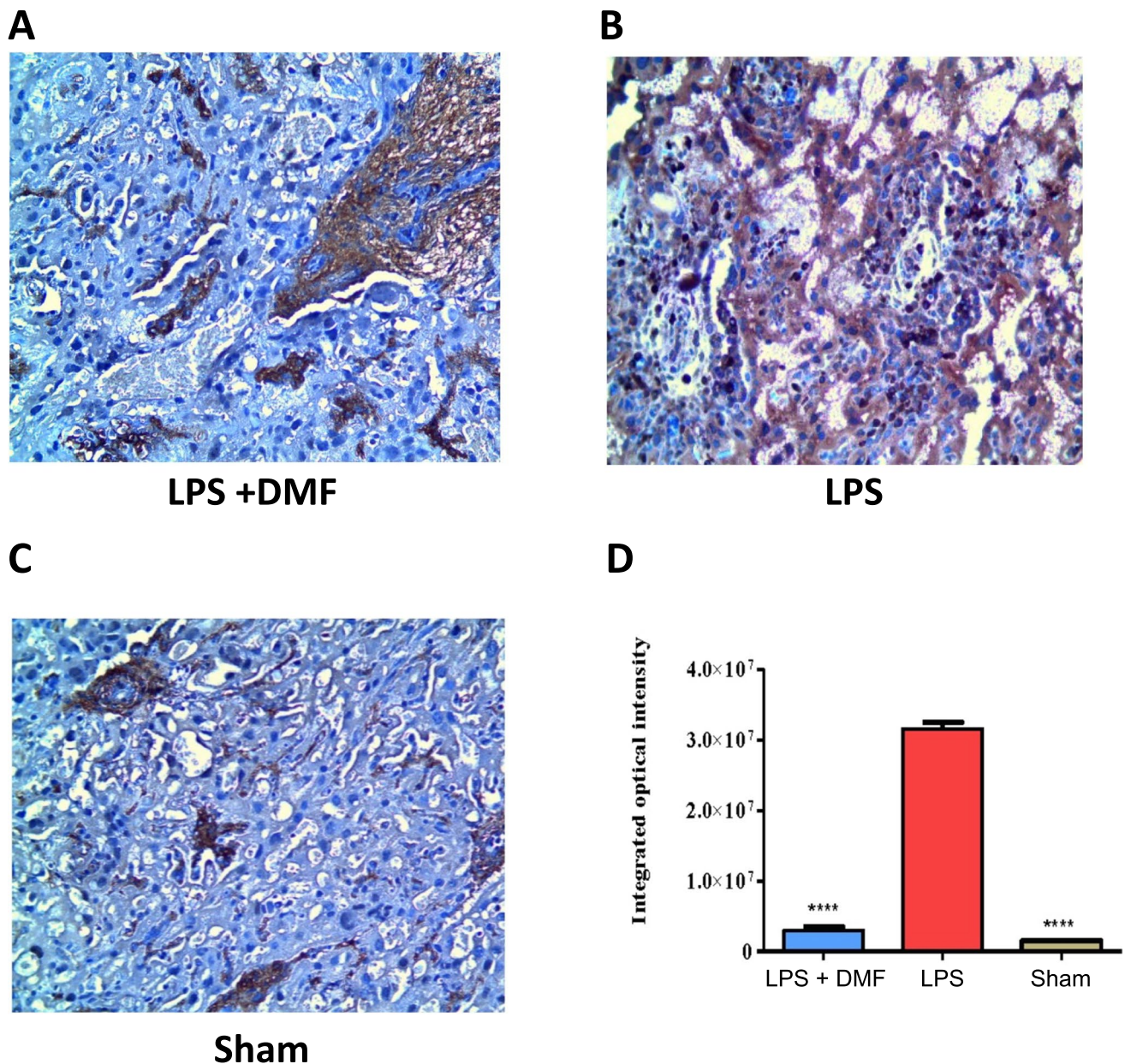


**Fig. 4** DMF attenuates IL-6 expression in the mouse placental labyrinth. One placenta per litter was randomly selected for immunohistochemistry from each of the **A**, DMA rescued (n=7); **B**, LPS (n=8); and **C**, sham (n=4) E16 dams. **A–C**, Representative sections reacted with primary IL-6 antibodies from each of the groups. **D**, Staining

intensity in the various groups, analyzed with Image-Pro Premier software. Original magnification 400X. The *quadruple asterisks* indicate  $P < .0001$ , as compared to the LPS group. *DMF*, N,N-dimethylformamide; *IL-6*, interleukin-6; *LPS*, lipopolysaccharide.

reducing NF- $\kappa$ B transcriptional activity (Figure 6, third row).

#### DMF Rescues Mice from LPS-Induced Preterm Birth

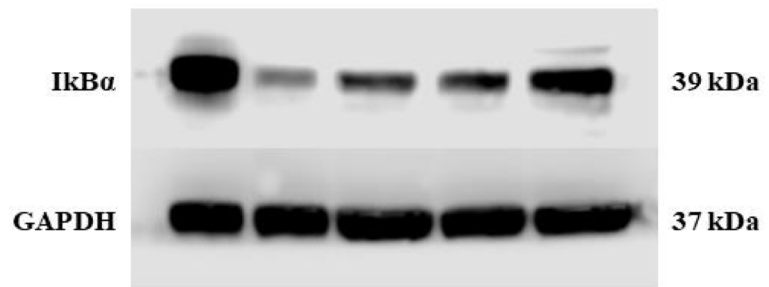
Based on the *in vitro* and *in vivo* histological data described above and on the structural similarity between DMF and DMA, we hypothesized that DMF would rescue LPS-challenged mice from developing preterm delivery.

All of the mice in the LPS group (n = 8) delivered within 24 h with a mean delivery time of  $t = 11$  h and 35 min (Table 1, Figure 7). Only one out of the seven mice in the DMF rescued group, however, delivered within the 24-h experimental period (at  $t = 10$  h), reflecting DMF's significant effect on PTB risk in our *in vivo* model (100% vs. 14.3%,  $P < .05$ , Table 1). As expected, none of the mice in the sham and DMF control groups delivered preterm. DMF had an even more significant effect on pups at risk

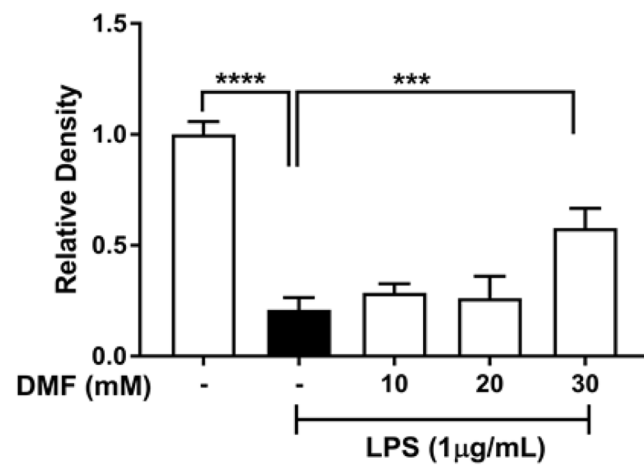


**Fig. 5** DMF specifically inhibits the NF- $\kappa$ B pathway. **A**, RAW 264.7 cells were stimulated with 1  $\mu$ g/mL of LPS for 15 min in the absence or presence of various concentrations of DMF, which was added to the media 2 h before the LPS. The effect of DMF on LPS-induced I $\kappa$ B $\alpha$  degradation was determined by immunoblotting with anti-I $\kappa$ B $\alpha$  antibody. **B**, Relative densities of I $\kappa$ B $\alpha$  expression bands were quantified using ImageJ. **C**, The effect of various concentrations of DMF on the MAPK pathway was tested by immunoblotting with various antibodies directed against MAPK pathway proteins, as indicated

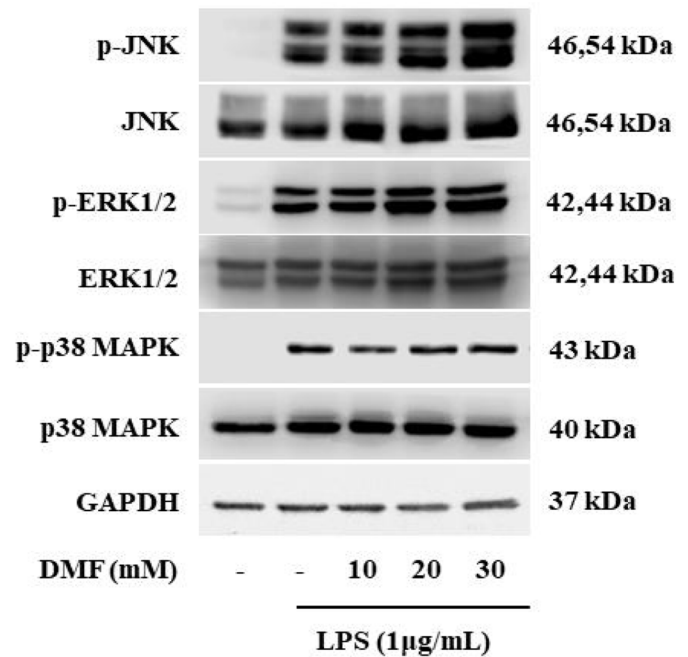
**A**



**B**



**C**



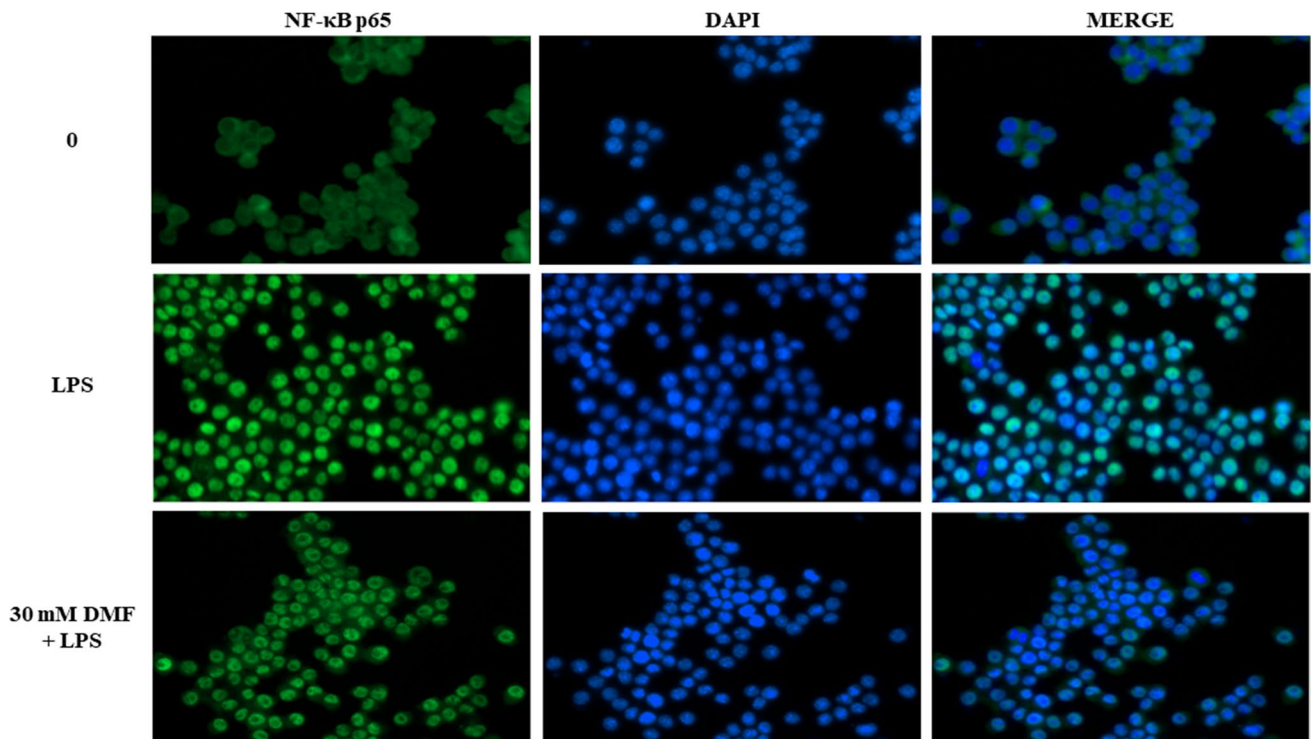


**Fig. 6** DMF prevents NF-κB nuclear translocation. RAW 264.7 cells were grown in the absence or presence of 30 mM DMF and then incubated for another 15 min with or without 1 μg/mL of LPS.

Immunostaining was carried out with fluorescent antibodies directed against the NF-κB p65 subunit (green), and DAPI was used to visualize nuclei (blue)

**Table 1** DMF delays preterm birth and rescues pups from preterm delivery

GROUPS	LPS	DMF Rescue	DMF Control	Sham
<b>Number of dams injected</b>	8	7	2	4
<b>Number of dams that delivered within 24 h</b>	8 (100%)	1* (14.3%)	0 (0%)	0 (0%)
<b>Total number of pups</b>	60	53	14	23
<b>Average total number of pups/litter</b>	7.5	7.6	7.0	5.8
<b>Number of pups delivered within 24 h</b>	38 (63.3%)	6**** (11.3%)	0 (0%)	0 (0%)
<b>Average number of pups/litter delivered within 24 h</b>	4.8 (63.3%)	0.9**** (11.3%)	0 (0%)	0 (0%)

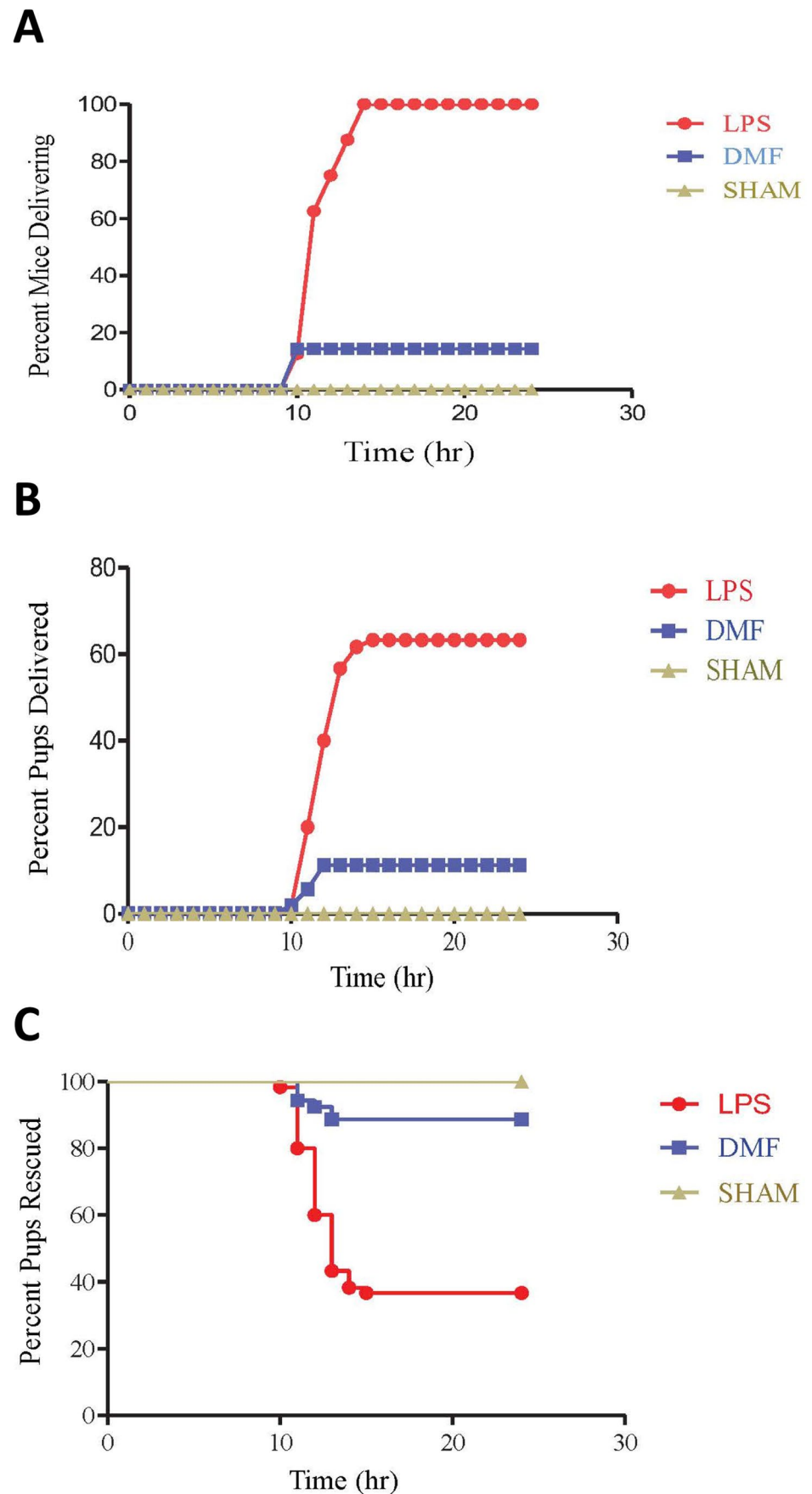
The asterisk indicates  $P < .05$ , and the quadruple asterisks indicate  $P < .0001$

of spontaneous PTB. While 38 of 60 (63.3%) pups were delivered within 24 h in the LPS group, all of which were non-viable, only 6 out of 53 (11.3%) pups were spontaneously aborted in the DMF rescued group ( $P < .0001$ , Table 1). The effect of DMF on LPS-challenged mice developing preterm labor and delivery over time is shown in Figure 5. Based on analysis by log-rank test (Mantel Cox), DMF has a significant effect on the rate of dams developing PTB ( $P < .0001$ , Figure 7, A), the rate of pups being spontaneously aborted ( $P < .0001$ , Figure 7, B) and, as illustrated by the Kaplan–Meier survival curve, the rate of pups being rescued ( $P < .0001$ , Figure 7, C).

## Discussion

In this report, using both *in vitro* and *in vivo* approaches, we show that DMF significantly decreases LPS-induced cytokine secretion from both macrophages and placental trophoblasts, cytokine expression in the placental labyrinth and immune cell infiltration at the maternal–fetal interface by specifically targeting the NF-κB pathway. Placental trophoblasts were included in the cytokine study, because *in vivo* they are accessible to DMF, which crosses the placenta, and like immune cells, they secrete cytokines.

**Fig. 7** DMF rescues mice from inflammation-driven preterm birth. DMF reduces **A**, the rate of LPS-challenged E15.5 mice delivering within 24 h ( $P < .0001$ ) and **B**, the rate of pups being spontaneously aborted in LPS-challenged E15.5 mice within 24 h ( $P < .0001$ ). **C**, The Kaplan–Meier plots show DMF’s ability to increase survival of pups in LPS-challenged mice over 24 h ( $P < .0001$ ). *DMF*, N,N-dimethylformamide; *LPS*, lipopolysaccharide



Finally, we show here, for the first time, that DMF delays inflammation-induced preterm birth without producing overt toxic effects.

This work was inspired by our ongoing interest in the potential of a related compound, DMA, as a novel drug therapy to prevent PTB. We have previously reported that 0.39 to 3.1 g/kg DMA delays PTB in LPS-induced E15.5 C57Bl/6 mice, that 0.2 to 3/1 g/kg DMA rescues pups from spontaneous delivery and that 1.56 g/kg DMA suppresses immune cell infiltration of the placental labyrinth [21]. In fact, DMF's anti-inflammatory and tocolytic efficacies are similar to those of DMA [21]. In additional work, we have determined that DMA prevents nuclear translocation of NF- $\kappa$ B and protects I $\kappa$ B $\alpha$ , the NF- $\kappa$ B inhibitory molecule that anchors it in the cytoplasm, from degradation, similar to the findings related to DMF's mechanism of action that we report here. Our work on DMA was corroborated by another group of investigators, who have also shown that this common drug excipient has anti-inflammatory effects mediated by inhibiting the NF- $\kappa$ B pathway [23].

Recent studies have shown that the anti-inflammatory properties exhibited by DMA extend to a group of aprotic solvents, which includes DMA and the structurally related molecule, N-methyl-2-pyrrolidone (NMP), both of which are, in turn, structurally related to DMF [21–24]. We were the first to show that DMA inhibits NF- $\kappa$ B *in vitro* and delays inflammation-driven PTB *in vivo* [21]. In the work presented here, we show that the closely related aprotic solvent, DMF, has anti-inflammatory efficacy by decreasing the levels of the cytokines TNF $\alpha$ , IL-6 and IL-8; inhibits NF- $\kappa$ B; and, specifically, delays inflammation-induced PTB *in vivo*. While we and others have described various mechanisms of action of DMA and NMP, which are structurally related to DMF, including inhibition of NF- $\kappa$ B [21–23], inhibition of the mitogen-activated protein kinase pathway [23] and inhibition of gene transcription by acting as bromodomain ligands [23, 24], the precise mechanism of action of DMF had not previously been reported.

As there are currently no FDA-approved drugs to arrest preterm labor, the discovery of a new anti-inflammatory compound that delays inflammation-driven birth is of significant clinical importance. Apart from its important effect on PTB risk, DMF's ability to decrease the levels of inflammatory cytokines has an additional significant benefit for the fetus, namely the prevention of fetal inflammatory response syndrome, which has been associated with elevated levels of IL-6 [29]. The elevated IL-6 levels in inflammatory response syndrome can result in several types of injury to the developing fetal brain, including cytokine-induced periventricular leukomalacia [30], hippocampal inflammation [31] and dysregulation of hippocampal glutamatergic homeostasis [31]. The fact that no overt toxic effects were observed in the dams or in the pups suggests that DMF is a promising

candidate for a novel tocolytic drug. Further toxicity studies followed by clinical trials are warranted to fully assess the efficacy and safety of this molecule.

This study has several important strengths. First, it addresses the urgent need for novel pharmacologic approaches to PTB, a serious clinical problem with no effective treatment [32–34]. Second, it includes both *in vitro* and *in vivo* methods to test our hypothesis. Third, it adds to the growing body of evidence that the DMA/DMF family of aprotic solvents has anti-inflammatory properties of potential clinical importance. Fourth, it shows that DMF's desirable anti-inflammatory properties are present at concentrations below cytotoxic levels *in vitro* and below toxic levels *in vivo*. A weakness of this study is that PTB was induced with a high dose of ip LPS which, while commonly used in PTB models, has questionable relevance to human pregnancy outside of sepsis and severe uterine infection. In addition, the ip route of administration of a drug, but typical of *in vivo* PTB models, would not be used clinically. The first DMF injection was administered before LPS was introduced, which does not represent a likely clinical scenario, unless a patient was known *a priori* to be at risk of infection or chorioamnionitis. The study is also limited by the fact that the dams were not allowed to continue their pregnancies beyond 24 hours after the LPS injections, so we do not know whether the DMF treatment would have led to the birth of viable offspring. Nor can we know whether those offspring would have been affected by the *in utero* DMF exposure and whether the pups would have had altered immune systems or other consequences. Finally, according to Manuel et al. (2017), *in vivo* models where PTB is brought on with LPS overemphasize the importance of infectious causes of PTB and ignore the diversity of PTB triggers in humans, including diet, environmental factors and other sources of oxidative stress [35]. *In vivo* models based on stressors other than LPS, such as oxidative stress, should be used more often by investigators in the PTB field.

The identification of a compound that has efficacy in preventing PTB without having toxic effects in the mother or fetuses has eluded the field until now. Of course, further investigation to ensure the safety of DMF before introducing the compound into clinical use is warranted. We and others have recently shown that vaginal nanoformulations can be used to take advantage of the uterine first pass and increase drug delivery to the uterus, while decreasing drug concentrations in the maternal systemic circulation and in the fetus [36–38]. This significant advance in the field opens the door for compounds that may have been previously rejected as potential drug therapy for PTB because of teratogenicity issues as well as for newly identified compounds that show promise in preclinical models, such as DMF.

Inflammation has been implicated in a wide range of human disorders, including cardiovascular disease [39,

40], cancer [41–44], neurodegenerative disorders [45–47] and of course PTB [10]. While pharmacotherapy exists for some of these medical challenges, many clinical needs related to inflammation remain unmet. In the USA, apart from inflammation resulting from infection, sterile inflammation is driven by dietary, environmental and even social factors. In fact, we have recently shown that consumption of a high-fat diet during pregnancy activates the oxidative stress/inflammatory axis [7, 26] and leads to increased rates of PTB in rodent models. The DMA/DMF family of aprotic solvents may represent a novel, safe, accessible and affordable approach to treat inflammation-driven preterm birth as well as other disorders resulting from inflammation for which existing drug therapy has not been fully efficacious.

**Supplementary Information** The online version contains supplementary material available at <https://doi.org/10.1007/s43032-022-00924-z>.

**Acknowledgments** This work was funded by a grant from the National Institutes of Health to SER (1R01NS069577). We are grateful to Helen Scaramell and the entire staff of the St. John's University Animal Care Center for maintenance of our mouse colony and assistance with *in vivo* protocols. We also thank Ms. Ernestine Middleton of Montefiore Medical Center, Bronx, NY, for her expert technical support in preparing the histology slides.

**Author Contributions** Z.-H. W. and O.O.S. performed all of the experiments and contributed equally to this manuscript. J.K. assisted in the performance of the *in vitro* experiments. S.M. assisted in the performance of the *in vivo* experiments. R.P. assisted with the statistical analyses. C.R.A. contributed to the original idea of the project and assisted with the writing of the manuscript. S.E.R. contributed to the original idea of the project, wrote the manuscript and provided funding.

**Data Availability** The data that support the findings in this study are available from the corresponding author upon reasonable request.

**Code Availability** N/A.

## Declarations

**Ethics Approval** Approval was obtained from the St. John's University IACUC, assurance number D16-00346 (A3574-01).

**Consent to Participate** N/A.

**Consent for Publication** N/A.

**Conflicts of Interest/Competing Interests** None of the authors has any conflicts to disclose.

## References

- Liu L, Oza S, Hogan D, et al. Global, regional, and national causes of under-5 mortality in 2000–15: An updated systematic analysis with implications for the Sustainable Development Goals. *Lancet*. 2016;388:3027–35.
- Blencowe H, Cousens S, Oestergaard M, Chou D, Moller AB, Narwal R, Adler A, Garcia CV, Rohde S, Say L, Lawn JE. National, regional and worldwide estimates of preterm birth. *Lancet*. 2012;379:2162–72.
- Martin JA, Osterman MJK. Describing the increase in preterm births in the United States, 2014–2016. National Center for Health Statistics 2018;Data Brief No. 312.
- Kerkhof G, Breukhoven PE, Leunissen RW, Willemsen RH, Hokken-Koelega AC. Does preterm birth influence cardiovascular risk in early adulthood? *J Pediatr*. 2012;161:390–6.
- Nuyt A, Lavoie JC, Mohamed I, Paquette K, Luu TM. Adult consequences of extremely preterm birth: cardiovascular and metabolic diseases risk factors, mechanisms, and prevention avenues. *Clin Perinatol*. 2017;44:315–32.
- Peelen MJ, Luef BM, Lamont RF, et al. The influence of the vaginal microbiota on preterm birth: A systematic review and recommendations for a minimum dataset for future research. *Placenta*. 2019;79:30–9.
- Manuel CR, Latuga MS, Ashby CR, Reznik SE. Immune tolerance attenuates gut dysbiosis, dysregulated uterine gene expression and high-fat diet potentiated preterm birth in mice. *Am J Obstet Gynecol*. 2019;220(596):e1–28.
- Salomon C, Nuzhat Z, Dixon CL, Menon R. Placental exosomes during gestation: liquid biopsies carrying signals for the regulation of human parturition. *Curr Pharm Des*. 2018;24:974–82.
- Menon R. Initiation of human parturition: signaling from senescent fetal tissues via extracellular vesicle mediated paracrine mechanism. *Obstet Gynecol Sci*. 2019;62:199–211.
- Keelan J. Intrauterine inflammatory activation, functional progesterone withdrawal, and the timing of term and preterm birth. *J Reprod Immunol*. 2017;125:89–99.
- Manuck TA. 17-alpha hydroxyprogesterone caproate for preterm birth prevention: Where have we been, how did we get here, and where are we going? *Semin Perinatol*. 2017;41:461–7.
- Caritis SN, Hauspurg A, Venkataramanan R, Lemon L. Defining the clinical response to 17-alpha-hydroxyprogesterone caproate. *Am J Obstet Gynecol*. 2018;219:623–5.
- O'Brien JM, Lewis DF. Prevention of preterm birth with vaginal progesterone or 17-alpha-hydroxyprogesterone caproate: A critical examination of safety and efficacy. *Am J Obstet Gynecol*. 2016;214:45–56.
- Heyborne KD, Allshouse AA, Carey JC. Does 17-alpha hydroxyprogesterone caproate prevent preterm birth in obese women? *Am J Obstet Gynecol*. 2015;213(844):e1–6.
- Co AL, Walker HC, Hade EM, Iams JD. Relation of body mass index to frequency of recurrent preterm birth in women treated with 17-alpha hydroxyprogesterone caproate. *Am J Obstet Gynecol*. 2015;213(233):e1–5.
- Lee LM, Liu LY, Sakowicz A, Bolden JR, Miller ES. Racial and ethnic disparities in use of 17-alpha hydroxyprogesterone caproate for prevention of preterm birth. *Am J Obstet Gynecol*. 2016;214(374):e1–5.
- Timofeev J, Singh J, Istwan N, Rhea D, Driggers RW. Spontaneous preterm birth in African American and Caucasian women receiving 17-alpha hydroxyprogesterone caproate. *J Matern Fetal Neonatal Med*. 2013;26:881–4.
- NCD Risk Factor Collaboration. Trends in adult body-mass index in 200 countries from 1975–2014: A pooled analysis of 1698 population-based measurement studies with 19.2 million participants. *Lancet*. 2016;387:1377–96.
- Mohamed SA, Thota C, Browne PC, Diamond MP, Al-Hendy A. Why is preterm birth stubbornly higher in African-Americans? *Obstet Gynecol Int J*. 2015;1:00019.
- Blackwell SC, Gyamfi-Bannerman C, Biggio JR, et al. 17-OHPC to prevent recurrent preterm birth in singleton gestations (PROLONG study): A multicenter, international, randomized double-blind trial. *Am J Perinatol*. 2019;37:127–36.

21. Sundaram S, Ashby CR, Pekson R, et al. N, N-Dimethylacetamide regulates the pro-inflammatory response associated with endotoxin and prevents preterm birth. *Am J Pathol.* 2013;183:422–30.
22. Pekson R, Poltoratsky V, Gorasiya S, Sundaram S, Ashby CR, Vancurova I, Reznik SE. N,N-Dimethylacetamide significantly attenuates LPS- and TNF $\alpha$ -induced proinflammatory responses via inhibition of the nuclear factor kappa B pathway. *Mol Med.* 2016;22:747–58.
23. Ghayor C, Gjoksi B, Dong J, Siegenthaler B, Caffisch A, Weber FE. N,N-Dimethylacetamide a drug excipient that acts as bromodomain ligand for osteoporosis treatment. *Sci Rep.* 2017;7:42108.
24. Chen TH, Weber FE, Malina-Altzinger J, Ghayor C. Epigenetic drugs as new therapy for tumor necrosis factor- $\alpha$ -compromised bone healing. *Bone.* 2019;127:49–58.
25. Vyas V, Ashby CR, Olgun NS, et al. Inhibition of sphingosine kinase prevents lipopolysaccharide induced preterm birth and suppresses pro-inflammatory responses in a murine model. *Am J Pathol.* 2015;185:862–9.
26. Williams L, Burgos E, Vuguin P, et al. N-Acetylcysteine resolves placental inflammatory-vasculopathic changes in mice consuming a high fat diet. *Am J Path.* 2019;189:2246–57.
27. Munnangi S, Gross SJ, Madankumar R, Reznik SE. Pregnancy associated plasma protein-A2: A novel biomarker for Down syndrome. *Placenta.* 2014;35:900–6.
28. Novembri R, De Clemente C, Funghi L, Torricelli M, Voltolini C, Challis JR, Petraglia F. Corticotropin releasing hormone and Urocortin 2 activate inflammatory pathways in cultured trophoblast cell line. *Eur J Obstet Gynecol Reprod Biol.* 2019;195:200–5.
29. Gomez R, Romero R, Ghezzi F, Yoon BH, Mazor M, Berry SM. The fetal inflammatory response syndrome. *Am J Obstet Gynecol.* 1998;179:194–202.
30. Kadhim H, Tabarki B, Verellen G, De Prez C, Rona AM, Sébire G. Inflammatory cytokines in the pathogenesis of periventricular leukomalacia. *Neurology.* 2001;56:1278–84.
31. Gisslen T, Singh G, Georgieff MK. Fetal inflammation is associated with persistent systemic and hippocampal inflammation and dysregulation of hippocampal glutamatergic homeostasis. *Pediatr Res.* 2019;85:703–10.
32. Muñoz-Pérez VM, Ortiz MI, Cariño-Cortés R, Fernández-Martínez E, Rocha-Zavaleta L, Bautista-Ávila M. Preterm birth, inflammation and infection: New alternative strategies for their prevention. *Curr Pharm Biotechnol.* 2019;20:354–65.
33. Reznik SE. Editorial: Novel pharmacotherapeutic targets and emerging approaches to preterm birth, Part 1. *Curr Pharm Des.* 2017;23:6097.
34. Reznik SE. Editorial: Novel pharmacotherapeutic targets and emerging approaches to preterm birth, Part 2. *Curr Pharm Des.* 2018;24:959.
35. Manuel CR, Ashby CR, Reznik SE. Discrepancies in animal models of preterm birth. *Curr Pharm Des.* 2017;23:6142–8.
36. Zierden HC, Ortiz JI, DeLong K, Yu J, et al. Enhanced drug delivery to the reproductive tract using nanomedicine reveals therapeutic options for prevention of preterm birth. *Sci Transl Med.* 2021;13:eabc6245.
37. Patki M, Giusto K, Gorasiya S, Patel K, Reznik SE. 17- $\alpha$ -Hydroxyprogesterone nanoemulsifying preconcentrate loaded vaginal tablet: A novel non-invasive approach for the prevention of preterm birth. *Pharmaceutics.* 2019;11:335. <https://doi.org/10.3390/pharmaceutics11070335>.
38. Giusto K, Patki M, Koya J, Ashby CR, Munnangi S, Patel K, Reznik SE. A vaginal nanoformulation of a sphingosine kinase inhibitor attenuates LPS-induced preterm birth in mice. *Nanomedicine (London).* 2019;14:2835–51.
39. Golia E, Limongelli G, Natale F, et al. Inflammation and cardiovascular disease: from pathogenesis to therapeutic target. *Curr Atheroscler Rep.* 2014;16:435.
40. Dai L, Golembiewska E, Lindholm B, Stenvinkel P. *Contrib Nephrol.* 2017;191:32–43.
41. Tuomisto AE, Mäkinen MJ, Väyrynen JP. Systemic inflammation in colorectal cancer: Underlying factors, effects and prognostic significance. *World J Gastroenterol.* 2019;25:4383–404.
42. Diakos CI, Charles KA, McMillan DC, Clarke SJ. Cancer-related inflammation and treatment effectiveness. *Lancet Oncol.* 2014;15:e493–503.
43. Coussens LM, Werb Z. Inflammation and cancer. *Nature.* 2002;420:860–7.
44. Balkwill F, Mantovani A. Inflammation and cancer: back to Virchow? *Lancet.* 2001;357:539–45.
45. Adams B, Nunes JM, Page MJ, et al. Parkinson's disease: A systemic inflammatory disease accompanied by bacterial inflammagens. *Front Aging Neurosci.* 2019;11:210.
46. Xu L, He D, Bai Y. Microglia-mediated inflammation and neurodegenerative disease. *Mol Neurobiol.* 2016;53:6709–15.
47. Fischer R, Maier O. Interrelation of oxidative stress and inflammation in neurodegenerative disease: role of TNF. *Oxidative Med Cell Longev.* 2015;2015:610813.

**Publisher's Note** Springer Nature remains neutral with regard to jurisdictional claims in published maps and institutional affiliations.